Shear-Induced Micellization of Diblock Copolymers

J. L. Jones,[†,‡] C. M. Marques,*[,†] and J.-F. Joanny[†]

Institut Charles Sadron, CNRS, 6 rue Boussingault, F-67083 Strasbourg, France, and Department of Physics, Polymer I.R.C., University of Leeds, Leeds LS2 9JT, United Kingdom

Received June 6, 1994; Revised Manuscript Received October 7, 1994[⊗]

ABSTRACT: The influence of a weak shear flow on the micellization of diblock copolymers in selective solvents is investigated. The micelles are described as small microgel beads and the hydrodynamic fields calculated within the Brinkman approximation. The critical micellar concentration is shown to decrease in the shear flow, leading to the possibility of shear-induced micellization. It is also shown that the aggregation number of the micelles is modified by the flow: it increases for micelles with a large asymmetry but decreases for more symmetric micelles.

1. Introduction

Diblock copolymers in a selective solvent behave as macromolecular analogues of low molecular weight surfactants.[1−5] Below the critical micellar concentration (cmc), only isolated chains are observed in the solution, while above this concentration almost all the chains belong to micellar aggregates. The isolated chains have a tadpole configuration, with a short collapsed head-block connected to a swollen tail. The micelles reproduce this structure on a larger scale: their core is a dense sphere of the nonsoluble blocks, while the outer corona can be viewed as a shell of swollen chains grafted to the central core. The heads of the tadpoles are the driving force for the aggregation: by sharing a common space with other chains in the center of the micelle, they reduce the number of their monomers exposed to the poor solvent. Aggregation leads however to a reduction of the total entropy of the system, and this is the predominant, energetically unfavorable effect at low concentrations. Only above the cmc does the enthalpic gain of the heads overcome the entropic losses and aggregates can form in solution.

Notwithstanding the strong similarities, copolymer solutions bare also a few marked differences with respect to usual surfactant systems. The large molecular dimensions of the collapsed chains in the tadpole head induce a very strong tendency to aggregate. This pushes the cmc toward small values that may sometimes be under the detection threshold.[2] These large dimensions are also important for the solvency of the copolymer, and it is quite clear that they impose a limit on the asymmetry values allowed for the diblock chains: if N_A is the number of monomers in the collapsed head and N_B the number of monomers in the swollen tail, one must roughly have $N_A \ll N_B^{3/2}$ in order to avoid precipitation.[6] Another important issue where the polymeric nature of the surfactants is relevant concerns micellization kinetics.[7−9] A very high selectivity of the solvent can lead to a glassy state of the cores; the micellar structure is then frozen and thus dependent on the preparation conditions. It is however believed that equilibrium can be achieved for cores which allow for some solvent penetration. In any case, the kinetic processes always involve exchange rates considerably smaller that the typical rates obtained for low molecular weight surfactant solutions.[2]

In this paper we study theoretically the steady state behavior of diblock copolymer micelles submitted to a weak hydrodynamic stress. This not only provides a tool for further understanding of the micellization mechanisms of copolymer chains but is also important from an experimental point of view. In many practical situations the micellar solutions are stirred, transported through tubes, filtered, etc., a number of situations where the dynamic state of the aggregate is dependent on the local flow rates to which it is subjected. We mimic these, more complex situations, by studying the behavior of a copolymer micelle in a simple shear flow. We follow closely the ideas developed by Brinkman for the treatment of a flow in a porous medium. In this approach, which has successfully been used in the past to discuss the hydrodynamics of related polymeric systems,[10−12] one treats the solvent flow through the micelle corona as the flow of a liquid through a porous medium with some local, and in principle position-dependent, permeability. The resulting flow is used to calculate the imposed deformation on the micelle structure, treated as an elastic medium surrounding the liquid core. These energetic contributions due to the shear allow then the prediction of the changes in the aggregation behavior induced by the flow.

The paper is organized as follows. In the next section we summarize the structural description and aggregation thermodynamics of diblock copolymer micelles. Section 3 gives a detailed hydrodynamic calculation of the effect of a shear flow on a spongelike object. As a pedagogical premise, we first review in this section the effect of a flow on a polymer-grafted layer, from which much insight can be gained into the more complicated problem of the spherical geometry. We then discuss the behavior of a spherical microgel with constant permeability and elastic modulus and finally give scaling laws for the behavior of the micelle in a shear flow. In Section 4 we incorporate the hydrodynamics results into the thermodynamic description and calculate the modifications induced by the flow on the different characteristics of the micellar solution: cmc, aggregation number, and micelle size. The final section is devoted to the discussion of the experimental relevance and limitations of our approach.

[†] Institut Charles Sadron.
[‡] University of Leeds.
[⊗] Abstract published in *Advance ACS Abstracts,* November 15, 1994.

0024-9297/95/2228-0136$09.00/0

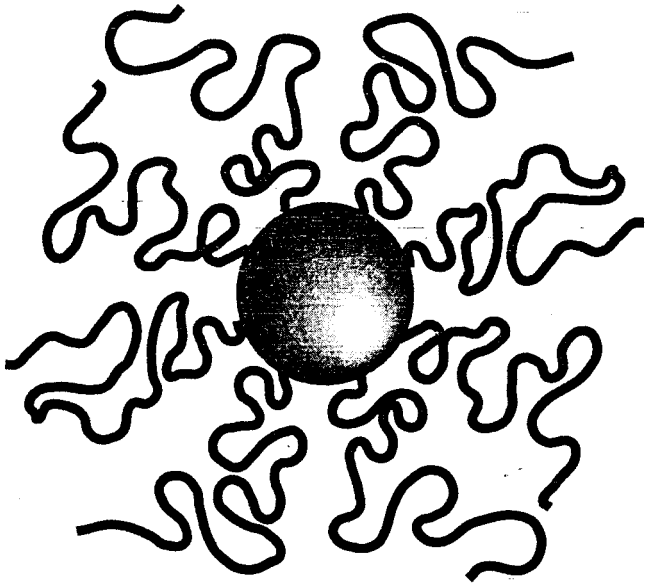

Figure 1. Sketch of the diblock copolymer micelle in a selective solvent. Its molten core results from the association of many collapsed blocks, and it is free of solvent. The chains in the outer corona form a starlike object where the chains follow locally the statistics of a semidilute polymer solution.

2. Micelles of Diblock Copolymers: Structure and Aggregation

In the following we consider asymmetric diblock copolymer chains, where the collapsed block of monomers in a poor solvent is much smaller than the swollen block. As shown elsewhere,[6] the relevant asymmetry range is given by the inequality $N_A \ll N_B^{15/11}$, N_A and N_B being the polymerization indices of the collapsed and swollen blocks, respectively. Throughout the paper, we assume that the insoluble block of the copolymer is in so poor a solvent that it has a tendency to form molten regions where neither the solvent nor the other block penetrates. The relaxation of this constraint, although important from a kinetic point of view for many experimental systems, is of little consequence for the thermodynamic picture described hereafter and can in principle be accounted for by a proper renormalization of the core–solvent interfacial tension.[5] Figure 1 depicts a representation of the structure of the micelle. Its central part is built from the many collapsed tadpole heads, and it is free of solvent. The incompressibility of the core leads to a simple relationship between the number p of chains in the micelle and the core radius: $R_A = (3pN_A/(4\pi))^{1/3}b$, where b is the size of one monomer. For simplicity we choose in the following a unit length where $b = 1$ and we assume that monomers A and B have equal sizes. The chains in the outer corona form a starlike object, a configuration first described by Daoud and Cotton.[13] In the corona the chains follow locally the statistics of a semidilute polymer solution. They can thus be described by a local, position-dependent correlation length. Pictorially one associates a blob with the correlation length and describes the external shell as a succession of blobs of increasing size. At a given distance r from the center of the micelle (with $r > R_A$), there are p blobs occupying a surface $4\pi r^2$. This gives a blob size which varies as $\xi(r) \simeq rp^{-1/2}$ (corrections to these scaling laws are discussed in the Appendix). The external radius of the micelle, R_B, is then obtained by the conservation constraint $pN_A = 4\pi\int_{R_A}^{R_B} c(r)r^2 dr$, where the monomer concentration in the corona decays as $c(r) \simeq p^{2/3}r^{-4/3}$. This gives $R_B = N_B^{3/5}p^{1/5}$. The chains in the core are thus extended by a factor $p^{1/5}$ with respect to their free radius in the solution. The free energy associated with these stretched configurations can be calculated by integrating the local free-energy density of an equivalent semidilute solution, $F_o = 4\pi k_B T\int_{R_A}^{R_B}\phi^{9/4}r^2 dr \simeq k_B T p^{3/2}\log[R_B/R_A]$.

In order to study the micellization of the diblock copolymer chains, one starts from the grand canonical potential for one micelle in equilibrium with a solution of free chains with a chemical potential μ

$$\Omega = F_o(p) + F_s(p) - \mu p \tag{1}$$

where $F_s = 4\pi k_B T\gamma R_A^2$ is the contribution to the free energy due to γ, the core–solvent interfacial tension (in $k_B T$ units). To a good approximation the chemical potential of the free chains can be written as $\mu = F_o(1) + F_s(1) + \log\phi$, where ϕ is the total volume fraction of copolymers in the solution. The aggregation numbers and the cmc are obtained from the two conditions $d\Omega/dp = \Omega = 0$. Approximating the logarithmic contribution to the osmotic energy as a constant A one gets

$$\begin{cases} p_0 = N_A^{2/5}\gamma^{6/5}\dfrac{4\pi}{3}\left(\dfrac{3}{\pi A^2}\right)^{3/5} \\ \mu_0 = N_A^{4/5}\gamma^{3/5}5\left(\dfrac{\pi A^2}{3}\right)^{1/5} \end{cases} \tag{2}$$

The critical micellar concentration is then obtained by setting $\mu = \mu_0$. The dominant contribution can be easily checked to give $\phi_{cmc} \sim \exp(-N_A^{2/3}\gamma)$.

3. Hydrodynamics

In this section, we study the velocity field around a micelle in a simple shear flow and investigate the deformation of the micelle induced by this velocity field. The micelle corona is permeable to the flow. The local friction between polymer and solvent couples the flow to the polymer conformations and induces an elastic deformation of the micellar corona. The flow through the micelle corona is studied here via the so-called Brinkman approximation[14] which has been introduced for the hydrodynamics of porous media. We use a two-fluid model where one of the fluids is the solvent and the other one is the polymer that acts as an elastic medium. For pedagogical purposes, we first study within the same approximations a simpler one-dimensional system which shares some similarity with the micelle: a grafted polymer layer in a shear flow. We then discuss the behavior of a spherical microgel with a constant pore size subjected to the shear flow for which the hydrodynamic equations can be solved without further approximations. The microgel is simpler than the micelle corona in the sense that the effective pore size and thus both the friction constant and the elastic modulus have constant values and do not vary with the distance from the center as in the case of a micelle. The results obtained for the microgels give sufficient insight into the problem to then allow the writing of scaling laws for the behavior of the micelle in a shear flow.

3.1 A Polymer Brush in a Shear Flow. We consider a grafted polymer layer, commonly designated as a brush, subjected to a shear flow. The chain ends are attached to the xz-plane, and the shear is applied in the x-direction. In the absence of the brush, the velocity of the fluid varies as $v_x = \dot{\gamma}y$. The grafted layer

is described here for simplicity by the Alexander de-Gennes model.[15,16] If the distance between grafting points is ξ, each chain in the layer can be viewed as an extended chain of blobs of size ξ and the local structure of the layer is the same as that of a semidilute polymer solution with a constant correlation length ξ. The elastic modulus E of the layer is of order $E \simeq k_B T/\xi^3$. We call L the total thickness of the layer.

In the region outside the brush, the velocity field satisfies the Stokes equation and the velocity increases linearly with the distance

$$v_x(z) = v_L + \dot{\gamma}(y - L) \tag{3}$$

where v_L is the velocity at the surface of the layer $y = L$.

For hydrodynamic purposes, we treat the polymer layer as a porous medium with a permeability of $1/\xi_H^2$ [12] where, as in a semidilute polymer solution, the hydrodynamic screening length ξ_H is proportional to the correlation length ξ. The velocity field inside the polymer layer satisfies the Brinkman equation

$$\eta\nabla^2\mathbf{v} - \frac{\eta}{\xi_H^2}\mathbf{v} = 0$$

where η is the solvent viscosity. In this equation the viscous flow is balanced by a "Darcy-like" term which describes well the flow of viscous liquids through porous media. At the surface of the brush, both the velocity and the tangential stress are continuous. On the solid surface there is no slip between the solvent and the wall and $v_x(0) = 0$. Using these boundary conditions, we obtain the velocity profile inside the layer

$$v_x(y) = v_L\frac{\sinh(y/\xi_H)}{\sinh(L/\xi_H)} \tag{4}$$

and the velocity at the brush surface

$$v_L = \xi_H\dot{\gamma}\tanh(L/\xi_H) \tag{5}$$

The flow only penetrates in the polymer brush over a very thin layer in the vicinity of the surface with a thickness equal to the hydrodynamic screening length ξ_H. Deeper in the polymer layer, the velocity vanishes exponentially. In the limit where the chains in the brush are highly stretched, $L \gg \xi_H$ and the velocity at the surface of the layer is $v_L = \xi_H\dot{\gamma}$. The hydrodynamic thickness of the polymer layer is therefore given by $L - \xi_H$.

For the micelle problem, we ultimately want to determine the elastic energy due to shear. This requires the determination of the elastic stress which is obtained from the force balance equation on the polymer

$$\nabla\cdot\sigma^E + \frac{\eta}{\xi_H^2}\mathbf{v} = 0 \tag{6}$$

At the surface of the polymer layer, the elastic stress vanishes and

$$\sigma_{yx}^E = \dot{\gamma}\eta\left(1 - \frac{\cosh(y/\xi_H)}{\cosh(L/\xi_H)}\right) \tag{7}$$

The elastic stress is small in the first layer of size ξ_H at the surface of the polymer layer and reaches then a constant value equal to the viscous stress outside the brush, $\sigma_{zx}^E = \dot{\gamma}\eta$. The elastic energy due to shear stored in the polymer layer per unit area is then

$$\Delta F_o = \sigma_{yx}^{E\,2}L/2E = \frac{(\dot{\gamma}\eta)^2\xi^3 L}{2kT} \tag{8}$$

3.2 Microgels in a Shear Flow. In order to get more insight into the spherical geometry which is of interest for the micelles, we now study the behavior of a spherical microgel in a shear flow. The microgel has a radius R and a constant mesh size ξ. As for the grafted polymer layer, the elastic moduli (the Lamé coefficients) are constant throughout the gel and of order kT/ξ^3. The permeability of the gel in the Brinkman approximation is written as η/ξ_H^2, where the hydrodynamic screening length ξ_H is proportional to the mesh size ξ.

The microgel is placed in a simple shear flow for which the velocity field at infinity is $v_x = \dot{\gamma}y$. The important difference between the microgel and the grafted layer is that the velocity for the microgel is not tangential to the surface but also has a radial component normal to the surface of the gel. The total strain rate can be decomposed into a symmetric and an antisymmetric part, $e_{ij}^T = e_{ij}^S + e_{ij}^A$. The antisymmetric part corresponds to an uniform rotation of the system at a constant velocity $\dot{\gamma}/2$. The gel also has a rotational motion at the same velocity, and this antisymmetric part has no influence on the elastic properties of the gel. We thus in the following ignore the pure rotation and consider only the pure straining motion characterized by the symmetric part of the strain rate tensor $e_{ij}^S = e_{ij}$. The strain rate has only two nonvanishing components, $e_{xy} = e_{yx} = \dot{\gamma}/2$.

Outside the gel sphere $r > R$, the velocity field satisfies the Stokes equation. We write the velocity as $v_i = v'_i + e_{ij}x_j$ and the pressure as $p = p' + p_0$ where the primed quantities correspond to the perturbations due to the gel. The Stokes equation reads

$$\nabla p' = \eta\nabla^2\mathbf{v}' \tag{9}$$

The pressure satisfies a harmonic equation, $\nabla^2 p' = 0$, and mass conservation imposes that $\nabla\mathbf{v}' = 0$. The solution of these equations are obtained along the same lines as that of Batchelor[17]

$$p' = C\eta e_{ij}\frac{x_i x_j}{r^5}$$

$$v'_i = e_{ij}x_j M(r) + e_{ik}x_i x_j x_k Q(r) \tag{10}$$

The form of the functions $M(r)$ and $Q(r)$ satisfying the equations of motion are $M(r) = D/r^5$ and $Q(r) = C/2r^5 - 5D/2r^7$. The integration constants C and D are obtained below from the boundary conditions at the surface of the gel.

Inside the gel we take into account the friction between the solvent and the gel by a Brinkman friction term:

$$\nabla\bar{p} = -\frac{\eta}{\xi_H^2}\bar{\mathbf{v}} + \eta\nabla^2\bar{\mathbf{v}} \tag{11}$$

The pressure still satisfies a harmonic equation. The symmetry of the problem imposes the following form for the velocity and pressure fields

$$\bar{v}_i = e_{ij}x_j\bar{M}(r) + e_{ik}x_ix_jx_k\bar{Q}(r)$$
$$\bar{p}_i = \eta\bar{C}e_{ij}x_ix_j + p_0 \qquad (12)$$

It is convenient to use in the following the hydrodynamic screening length ξ_H as the unit length; in these units the radius of the gel is $a = R/\xi_H$. The homogeneity of the formulas can then be reestablished in the final result. Inserting the form 12 into the Brinkman equation leads to the following second-order equations for the functions $\bar{Q}(r)$ and $\bar{M}(r)$ inside the gel:

$$\frac{d^2\bar{Q}(r)}{dr^2} + \frac{8}{r}\frac{d\bar{Q}(r)}{dr} - \bar{Q}(r) = 0 \qquad (13)$$

$$\frac{d^2\bar{M}(r)}{dr^2} + \frac{4}{r}\frac{d\bar{M}(r)}{dr} - \frac{\bar{Q}(r)}{r} + 4\bar{Q}(r) = 0 \qquad (14)$$

These equations are solved by imposing that the velocity is finite at the origin and thus that both $\bar{Q}(r)$ and $\bar{M}(r)$ are finite at the origin. Mass conservation also imposes that $\nabla\cdot\bar{\mathbf{v}} = 0$. The functions $\bar{Q}(r)$ and $\bar{M}(r)$ are then found to be

$$\bar{Q}(r) = Vr^{-4}\left(\cosh(r)\left(1 + \frac{15}{r^2}\right) - 3\sinh(r)\left(\frac{2}{r} + \frac{5}{r^3}\right)\right)$$

$$\bar{M}(r) =$$
$$-2\bar{C} + V\sinh(r)\left(\frac{6}{r^5} + \frac{3}{r^3}\right) + V\cosh(r)\left(-\frac{6}{r^4} - \frac{1}{r^2}\right) \qquad (15)$$

This gives the velocity field for a permeable sphere in a simple shear flow as a function of the four integration constants C, $\bar{C}$, V, and D. In order to find these integration constants, we focus on the case where the size R of the gel is much larger than the mesh size ξ_H, i.e., where the dimensionless size a is larger than 1. In the vicinity of the surface of the gel, we can approximate $\bar{Q}(r) \simeq V\exp(r)/(2r^4)$ and $\bar{M}(r) \simeq -2\bar{C} - V\exp(r)/(2r^2)$. The four integration constants are then found by writing the continuity of the velocity and of both the normal and tangential components of the stress at the interface between the gel and the pure solvent. Note that these conditions are different from the ones used by Batchelor[17] to study the motion of a liquid sphere embedded in a pure straining motion. The four integration constants are then $C \simeq -5a^3$, $D \simeq -a^5$, $\bar{C} \simeq -5/a^2$, and $V \simeq -10a\exp(-a)$.

In order to illustrate these results, we have plotted in Figure 2 the component v_x of the velocity when $x = 0, z = 0$ as a function of the radius r. The velocity on the surface is as for the brush of order $\simeq\dot{\gamma}\xi_H$. The main difference with the planar problem where the velocity is tangential to the surface of the brush is that for the microgel the velocity does not decay exponentially to zero. It is the sum of two components, a component that decays exponentially from the surface over the hydrodynamic screening length ξ_H and a component that increases linearly from the center of the gel. This linear component is always finite, and there is thus always flow inside the gel. However the ratio of this linear component to the total velocity around the surface of the gel is of the order $1/a$ and the linear component can be safely neglected in the limit where a is large. Qualitatively we thus obtain a result very similar to that obtained in the planar geometry, the flow only penetrates inside the gel over a thin layer of size ξ_H around the surface.

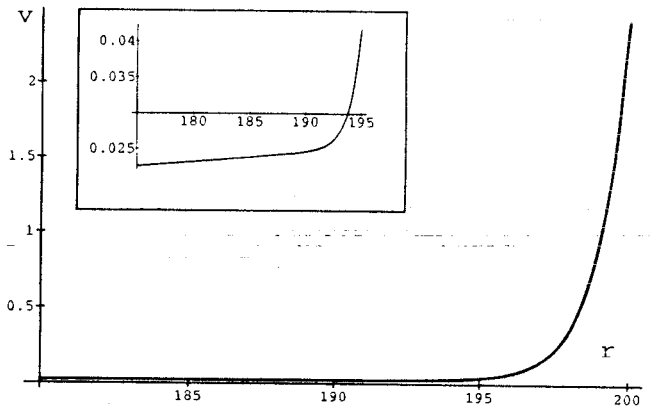

Figure 2. v_x component of the velocity when $x = 0, z = 0$ as a function of r, the microgel radius in units of the hydrodynamic screening length. For the spherical microgel, the velocity does not decay exponentially to zero (see inset). It is the sum of two components, a component that decays exponentially from the surface over the hydrodynamic screening length ξ_H and a component that increases linearly from the center of the gel. However, this linear component, which implies that there is always flow inside the microgel, has a small magnitude and can be neglected.

Inside the gel, the Brinkman friction force is balanced by an elastic deformation and in a steady state elastic energy is stored. The elastic stress is obtained from eq 6. The symmetry of the problem imposes for the displacement u_i the same functional form as that of the velocity profile

$$u_i = e_{ij}x_jA(r) + e_{kl}x_ix_kx_lB(r) \qquad (16)$$

The gel is an isotropic elastic medium with two independent elastic moduli. We use here the two Lamé coefficients λ and μ which are both of the order k_BT/ξ^3. The elastic stress then reads

$$\sigma_{ij} = 2\mu\mu_{ij} + \lambda u_{kk}\delta_{ij} \qquad (17)$$

where $u_{ij} = {}^1/_2(\partial u_i/\partial x_j + \partial u_j/\partial x_i)$ is the deformation. The force balance on the gel can be written as

$$\mu\nabla^2 u_i + \frac{\partial P}{\partial x_j} = \frac{v_i\eta}{\xi_H^2} \qquad (18)$$

where $P = (\lambda + \mu)u_{kk}$ plays the role of a pressure. This pressure satisfies a harmonic equation, $\nabla^2 P = 0$. It is thus given by $P = Ge_{ij}x_ix_j = G\dot{\gamma}xy$, where G is an integration constant. The force balance equation gives the following coupled equations for the functions $A(r)$ and $B(r)$.

$$\frac{d^2B(r)}{dr^2} + \frac{8}{r}\frac{dB(r)}{dr} + \frac{\eta\bar{Q}(r)}{\mu} = 0$$

$$\frac{d^2A(r)}{dr^2} + \frac{4}{r}\frac{dA(r)}{dr} + 4B(r) = \frac{\eta M(r)}{\mu} - \frac{2G}{\mu} \qquad (19)$$

where, as above, we have used the hydrodynamic screening length ξ_H as unit length. In the vicinity of the surface of the gel, the solutions for $A(r)$ and $B(r)$ are

$$B(r) = B_0 - \frac{\eta V \exp(r)}{2\mu r^4}$$

$$A(r) = A_0 + \frac{r^2}{10\mu}(-2C + 2\bar{C}\eta - 4B_0\mu) + \frac{\eta V \exp(r)}{2\mu r^2} \quad (20)$$

This gives the displacement for each point of the gel with three unknown constants, A_0, B_0, and G. The constants A_0, B_0, and G are evaluated from the two boundary conditions: (i) the stress is everywhere zero at the surface $\sigma_{ij}n_j = 0$ and (ii) $u_{kk} = P/(\lambda + \mu)$. Assuming that $a = R/\xi_H \gg 1$, we obtain the leading terms in the constants $A_0 \simeq \eta/\mu$, $B_0 \simeq \eta/(\mu a^2)$, and $G \simeq -\eta/a^2$.

All the components of the elastic stress can now be determined from $\sigma_{ij} = 2\mu u_{ij} + \lambda u_{kk}\delta_{ij}$. This is a rather tedious task that we pursue only qualitatively at the level of scaling laws. The elastic stress vanishes at the surface of the gel and remains small in a thin shell of thickness ξ_H close to the surface. Over the remaining volume of the gel, the elastic stress can be written as $\sigma_{ij} = \dot{\gamma}\eta f_{ij}(r/R)$ where f_{ij} is a smooth function of order 1.

The elastic energy stored in the microgel is then estimated as

$$\Delta F_o \simeq (\dot{\gamma}\eta)^2 \xi^3 R^3/k_B T \quad (21)$$

Note that this expression is very similar to that obtained for the grafted layer.

3.3 A Spherical Micelle under Shear. We now come back to the behavior of a starlike micelle in a shear flow. The corona of the micelle acts as an elastic porous medium and thus has a behavior very similar to the mesogel with the difference that the hydrodynamic screening length is not a constant but increases linearly with the distance from the center of the micelle. Since the friction between polymer and solvent gets higher as one gets toward the center, the penetration of the flow in the corona occurs only over one hydrodynamic screening length around the outside of the micelle. The hydrodynamic screening length is of the order of the size of the largest blob in the Daoud–Cotton construction $\xi(R_B)$, and the velocity at the surface of the micelle is of the order $v \simeq \dot{\gamma}\xi(R_B)$. As for the microgel, the elastic stress varies only very smoothly over the volume of the corona and is of the order $\sigma \simeq \dot{\gamma}\eta$.

The elastic energy stored in the micellar corona due to the shear is

$$\Delta F_o = \int \frac{\sigma^2}{E(r)} d\mathbf{r}$$

where the modulus E is radius dependent, $E \propto k_B T/\xi(r)^3$, and $\xi = rp^{-1/2}$. The integral is dominated by the largest values of the radius $r \simeq R_B$, and the elastic energy is still given by eq 21 where the relevant blob size is $\xi(R_B)$ and $R = R_B$.

The stress is transmitted by the elasticity of the chains forming the corona to the core of the micelles which deforms as a liquid droplet subjected to an external shear. For a given volume of the core, the deformation is associated with an increase of the area and thus with an increase of the interfacial energy of the core. We estimate the deformation of the core of the micelle qualitatively using the Taylor theory[18] for the deformation of liquid droplets in a shear flow. Within this theory, which balances the viscous and Laplace stresses at the surface of the droplets, the spherical core is in a first approximation deformed into an ellipsoid with longer and smaller axis, a and b, respectively. A droplet submitted to a stress σ has an anisotropy $(a - b)/(a + b) \simeq \sigma R_A/\gamma$, where R_A is the radius of the core of the micelle. For a given volume, the sphere is the surface with the smallest area and the change in area due to the deformation is proportional to the square of the anisotropy. We therefore obtain a change in interfacial free energy,

$$\Delta F_s = k_B T \gamma R^2{}_A (\sigma R_A/\gamma k_B T)^2 = \frac{(\dot{\gamma}\eta)^2 R^4{}_A}{\gamma k_B T} \quad (22)$$

where we have used the value of the elastic stress at the surface of the core $\sigma \simeq \dot{\gamma}\eta$.

4. Effect of Shear on Micellization

We study in this section a solution of diblock copolymers under a given applied shear rate. Although this is not a system at thermal equilibrium, we consider here only small shear rates and thus systems close to thermodynamic equilibrium, and we describe the aggregation behavior by an effective thermodynamic potential,

$$\Omega(p) = \Omega(p,\dot{\gamma} = 0) + \Delta F_o(p,\dot{\gamma}) + \Delta F_s(p,\dot{\gamma}) \quad (23)$$

where the shear-dependent contributions to the effective potential have been calculated in the previous section and can be written as

$$\Delta F_o(p,\dot{\gamma}) = (\dot{\gamma}\tau_\xi)^2 \quad F_o(p) = (\dot{\gamma}\tau_z)^2 p^{-9/5} F_o(p)$$

$$\Delta F_s(p,\dot{\gamma}) = (\dot{\gamma}\tau_\gamma)^2 \quad F_s(p) = (\dot{\gamma}\tau_t)^2 p^{2/3} F_s(p) \quad (24)$$

There are essentially two different characteristic times involved in these expressions. The first one is the Zimm time of the largest blob in the micelle corona

$$\tau_\xi = \frac{\eta \xi (R_B)^3}{k_B T} \quad (25)$$

The Zimm time[19] of a polymer chain, τ_z, of N_B monomers (such as the arms of the starlike micelle) is the longest relaxation time of the hydrodynamic relaxation spectrum of the chain in a solvent and scales as the cube of the polymer dimensions $\tau_z \simeq N_B^{9/5}$. The Zimm time of the largest blob τ_ξ is thus smaller than τ_z by a factor of $p^{9/10}$, indicating that the chains in the micelle are less distorted by the flow than the isolated chains in the solution. We have used here the Daoud–Cotton model for the chains in the corona where there is a factor of $p^{3/10}$ between the dimensions of the last blob and the dimensions of the nonassociated chain. This model is however based on the assumption that all the end points of the chains are on the outside of the corona as in the Alexander model of polymer brushes. This may underestimate the size of the largest blob; in the Appendix we give a better estimation of the size of the last blob.

The second important time is the relaxation time of a liquid droplet in a shear flow. This time, which depends of course on the size of the droplet, is mainly controlled by the ratio of the viscosity to the interfacial tension of the droplet

$$\tau_\gamma = \frac{\eta R_A}{\gamma k_B T} \tag{26}$$

It is clear from eq 26 that the Taylor time τ_γ associated with the core of one micelle is larger by a factor of $p^{1/3}$ than the corresponding time, $\tau_t = \eta N_A^{1/3}/\gamma k_B T$, for the relaxation of the collapsed head of one isolated copolymer chain. The Taylor distortion energy *per chain* is therefore larger for a copolymer head in the core than for the head of an isolated copolymer in the sheared solution. In the last section we will see that this effect is determinant for micelles with small asymmetries.

The two calculated contributions for the effective, shear-dependent potential have very different orders of magnitude. At equilibrium, the ratio of the two times is

$$\tau_\xi/\tau_\gamma \simeq (R_B/R_A)^3 \gg 1 \tag{27}$$

For the whole range of parameters considered, the contribution from the core distortion can be neglected, and the thermodynamic potential reduces to the form $\Omega(p) = \Omega(p,\dot\gamma = 0) + \Delta F_o(p,\dot\gamma)$. The shifts in aggregation number and chemical potential can be calculated pertubatively, by setting $p = p_0 + \Delta p$ and $\mu = \mu_0 + \Delta\mu$ and solving the equilibrium conditions $d\Omega/dp = \Omega = 0$. One gets

$$\Delta\mu = \frac{\Delta F_o}{p_0};\ \Delta p = -\frac{p_0 \frac{d\Delta\mu}{dp_0}}{\frac{d^2F_o}{dp_0^2}} \tag{28}$$

The change induced to the chemical potential at the cmc is, perturbatively, given by the change of the energy per chain in the micelle. The sign of the chemical potential shift is therefore dependent on the sign of the added perturbation. In our case the flow always increases the distortion of the chains, thus leading to an increase of the chemical potential at the cmc: $\Delta\mu \simeq \mu_0(\dot\gamma\tau_\xi)^2$. However, the reference contribution to the chemical potential $F_0(1)$ is also shifted by the flow. This contribution is larger and leads to a *decrease* of the cmc

$$\phi_{cmc}(\dot\gamma) = \phi_{cmc}(\dot\gamma = 0)\exp[-\Delta F_o(\dot\gamma, p = 1)] \tag{29}$$

where ΔF_o is obtained from eqs 24 by setting $p = 1$. For small shear rates, the shift in the cmc can be described by a parabolic shape, $\phi_{cmc}(\dot\gamma) = \phi_{cmc}(\dot\gamma = 0) \times [1 - (\dot\gamma\tau_z)^2]$, which depends only on the Zimm time of the isolated chains in solution. Note that, because the critical micellar concentration is decreased by the flow, the micellization can be induced by an applied shear flow. This situation bares some similarities with shear-induced phase transitions,[20-22] where an ordered phase may be nucleated from a disordered phase by applying a shear flow.

The aggregation number of the micelles is modified by the flow in a more subtle manner: it depends both on the sign of the added energy contribution per chain and on its dependence with the number of chains in the micelle. In our case, the energy is increased by the flow but the effect of flow distortion on the micelle chains decreases with chain number, thus resulting on a net increase of the aggregation number. We get

$$\frac{\Delta p}{p_0} \simeq (\dot\gamma\tau_\xi)^2 \tag{30}$$

with the largest blob size evaluated for a nondistorted micelle. This result can be understood simply by noting that the distortion energy per chain is smaller for large micelles than for small ones. The chains thus tend to build larger aggregates in order to avoid the energy penalty associated with elastic distortion.

5. Discussion

In the present work we have studied the formation of micelles of diblock copolymers subjected to a shear flow. The micelles have been considered as small spongelike spheres, and the flow was calculated following the Brinkman approximation. Within this approximation, where the pressure losses are proportional to the flow rates (Darcy law for porous media), we rigorously derived the velocity and stress fields outside and inside the porous sphere. The hydrodynamic section of our results is therefore quite general and could in principle be used to determine the flow characteristics of other similar physical systems, as for instance microgel beads or agglomerates of small colloidal particles. An extension of our work could also provide the corrections to the Stokes–Einstein law for the diffusion coefficient of small "spongelike" objects in suspension.

From the point of view of micellization, the important information provided by the hydrodynamics is the stress field, which allows to calculate the distortion imposed by the flow on the chains and thus the stored elastic energy. The association behavior has been described by an effective thermodynamic potential which is dominated by the shear-dependent stored elastic energy. We find that the aggregation number of the micelles in the flow is increased. This can be understood by remarking that when the number of chains in the micelle increases, the distortion imposed by the flow on each chain decreases; the rigidity of the micelle increases with aggregation number. The chains tend thus to aggregate into larger micelles, in order to avoid distortion. Another important consequence of this effect is the decrease of the critical micellar concentration. Interestingly, this implies that micelles can be obtained by shearing a diblock copolymer solution below the cmc, a phenomenon which carries some similarities with shear-induced order observed in other polymer systems.[20-22]

We considered only in this paper micelles of diblock copolymers in the asymmetry range $N_A \ll N_B^{15/11}$. Spherical micelles of these copolymers are however predicted[6] to form until N_A becomes of the order of $N_B^{3/2}$ where a dense lamellar phase appears. In the intermediate regime $N_B^{15/11} \ll N_A \ll N_B^{3/2}$, the thickness of the external corona is smaller than the core radius, and the dominant contribution from the flow can be easily checked to be the Taylor contribution of eq 22. The consequences of the imposed flow on the behavior of the micelles in this asymmetry regime bear some similarities with the ones described above for the more asymmetric micelles where the elastic distortion energy of the corona dominates. For instance, the shift of the critical micellar concentration is still given by eq 29 because the major effect is still the distortion of the solvated part of the tadpoles. However, the aggregation number in this regime is predicted to decrease. Indeed, the Taylor contribution per chain $\Delta F_s/p_0$—see eq 24—increases with chain number: by reducing their sizes, the micelles avoid better the flow distortion. We find

$$\frac{\Delta p}{p_0} \simeq -(\dot{\gamma}\tau_\gamma)^2 \tag{31}$$

Our results are limited to shear rates smaller than the characteristic Zimm time for a polymer chain of the size of the last blob in the micellar corona. The corresponding rates are far too high to envisage a classical shearing experiment in a viscosimeter; they are comparable to the actual shear rates in small capillaries or filtering membranes. This suggests that they are relevant in many practical situations, and we hope that our preliminary theoretical results will encourage a systematic study of these effects. An interesting study that came to our knowledge during the reviewing process[23] was conducted by Antonietti et al. on poly(styrene)/poly(4-vinylpyridine) block copolymers. Their results indicate that micelles desaggregate under shear, in contradiction with our predictions for the relevant asymmetry range of the considered diblock copolymers. However, even the static results disagree with the scaling predictions for the aggregation numbers at thermodynamic equilibrium, rendering very difficult any testing of the dynamical behavior. In our opinion, the issue that is at stake here is the possibility of really attaining thermodynamic equilibrium conditions for the cores of the micelles. The aggregation of tadpole molecules with a glassy head, for instance, would certainly lead to very different results.

Acknowledgment. J.L.J. is grateful to Elf-Atochem for financial support. We also thank R. Zana (I.C.S. Strasbourg) for fruitful discussions.

Appendix

Throughout the paper, we have described the corona of the micelle by the Daoud–Cotton blob model. This is a spherical version of the Alexander blob model for planar polymer brushes, and it implicitly assumes that all the end points of the chains are on the outside of the starlike micelle. It is known that this is not actually the case and that many end points are buried deep inside the star. For a planar grafted layer, the end point density can be taken into account by the so-called self-consistent field model. In the spherical geometry, one can work at the level of scaling laws and divide the star corona into two regions. The inner part contains a finite fraction of the monomers and is well-described by the Daoud–Cotton model. The radius of the inner part is a finite fraction of the total radius $R_B \simeq p^{1/5}N_B^{3/5}$. The outside part of the star can be considered as an (almost) planar brush with a grafting density (number of chains per unit area) $\sigma = p/R^2_B$. The overall size of the corona remains the same as in the Daoud–Cotton model, and the elastic free energy is dominated by the inner part and is still $F_0 = k_BTp^{3/2}$.

For a planar brush in a good solvent, the size of the largest blob, i.e., the concentration correlation length at the edge of the layer, has been calculated in ref 24 and is equal to

$$\xi(R_B) = N_B^{3/5}(\sigma N_B^{6/5})^{-1/6} \tag{32}$$

For the starlike corona, we thus obtain the size of the last blob

$$\xi(R_B) = \frac{R_B}{p^{3/10}} = N_B^{3/5}p^{-1/10} \tag{33}$$

All the results obtained for the micelle in a shear flow in the Daoud–Cotton model can still be used qualitatively with this value for the size of the largest blob. In particular, the elastic free energy due to the shear stored in the corona is still given by eq 21, $\Delta F_0 = (\dot{\gamma}\eta)^2\xi^3R^3_B/k_BT = (\dot{\gamma}\tau_{el})^2 F_o(p) = (\dot{\gamma}\tau_z)^2 p^{-6/5}F_o(p)$, where the relevant time for the elastic deformation of the corona is slightly larger than in the Daoud–Cotton model, $\tau_{el} = \tau_z p^{-3/5}$.

This change in the scaling laws does not change qualitatively our conclusions. The aggregation number of the micelle under shear is larger than that of the equilibrium micelle with an increase of $\Delta p/p_0 = (\dot{\gamma}\tau_{el})^2$, and the critical micelle concentration decreases and is still given at lowest order in the shear rate by (29).

References and Notes

(1) Gallot, Y.; Franta, E.; Rempp, P.; Benoit, H. *J. Polym. Sci.* **1964**, *4*, 473.
(2) Tuzar, Z.; Kratochvil, P. *Adv. Colloid Interface Sci.* **1976**, *6*, 201.
(3) Vagberg, L. J. M.; Cogan, K. A.; Gast, A. P. *Macromolecules* **1991**, *24*, 1670.
(4) Halperin, A. *Macromolecules* **1987**, *20*, 2943.
(5) Marques, C. M.; Joanny, J. F.; Leibler, L. *Macromolecules* **1988**, *21*, 1051.
(6) Izzo, D.; Marques, C. M. *Macromolecules* **1993**, *26*, 7189.
(7) Tuzar, Z. *Macromol. Rep.* **1992**, *A29*, 173.
(8) Halperin, A.; Alexander, S. *Macromolecules* **1989**, *22*, 2403.
(9) Johner, A.; Joanny, J. F. *Macromolecules* **1990**, *23*, 5299.
(10) de Gennes, P. G. *Macromolecules* **1981**, *14*, 1637.
(11) de Gennes, P. G. *Adv. Colloid Interface Sci.* **1987**, *27*, 189.
(12) Fredrickson, G. H.; Pincus, P. A. *Langmuir* **1991**, *7*, 786.
(13) Daoud, M.; Cotton, J. P. *J. Phys. (Paris)* **1982**, *43*, 531.
(14) Brinkman, H. C. *Appl. Sci. Res.* **1947**, *A1*, 27.
(15) Alexander, S. *J. Phys. (Paris)* **1977**, *38*, 983.
(16) de Gennes, P. G. *J. Phys. (Paris)* **1976**, *37*, 1443.
(17) Batchelor, G. K. *An Introduction to Fluid Mechanics*; Cambridge University Press: Cambridge, 1967.
(18) Taylor, G. I. *Proc. R. Soc. London, A* **1879**, *29*, 71.
(19) Doi, M.; Edwards, S. F. *The Theory of Polymer Dynamics*; Clarendon Press: Oxford, 1986.
(20) Cates, M. E.; Milner, S. T. *Phys. Rev. Lett.* **1989**, *62*, 182.
(21) Marques, C. M.; Cates, M. E. *J. Phys. (Paris)* **1990**, *51*, 1733.
(22) Koppi, K. A.; Tirrell, M.; Bates, F. S. *Phys. Rev. Lett.* **1993**, *70*, 1449.
(23) Antonietti, M.; Heinz, S.; Schmidt, M.; Rosenauer, C. *Macromolecules* **1994**, *27*, 3276.
(24) Wijmans, C. M.; Zhulina, E. B. *Macromolecules* **1993**, *26*, 7214.

MA941019N